

Accepted Article Preview: Published ahead of advance online publication



Differential mode-gain equalization via femtosecond laser micromachining-induced refractive index tailoring

Cong Zhang, Senyu Zhang, Yan Zeng, Yue Wang, Meng Xiang, Di Lin, Songnian Fu and Yuwen Qin

Cite this article as: Cong Zhang, Senyu Zhang, Yan Zeng, Yue Wang, Meng Xiang, Di Lin, Songnian Fu and Yuwen Qin. Differential mode-gain equalization via femtosecond laser micromachining-induced refractive index tailoring. *Light: Advanced Manufacturing* accepted article preview 06 March 2024; doi: 10.37188/lam.2024.014

This is a PDF file of an unedited peer-reviewed manuscript that has been accepted for publication. LAM are providing this early version of the manuscript as a service to our customers. The manuscript will undergo copyediting, typesetting and a proof review before it is published in its final form. Please note that during the production process errors may be discovered which could affect the content, and all legal disclaimers apply.

Received 25 August 2023; revised 27 February 2024; accepted 05 March 2024;
Accepted article preview online 06 March 2024

Differential mode-gain equalization via femtosecond laser micromachining-induced refractive index tailoring

Cong Zhang^{1,2,3}, Senyu Zhang⁴, Yan Zeng¹, Yue Wang¹, Meng Xiang^{1,2,3}, Di Lin^{1,2,3}, Songnian Fu^{1,2,3}*, and Yuwen Qin^{1,2,3}

¹ Institute of Advanced Photonics Technology, School of Information Engineering, Guangdong University of Technology, Guangzhou, 510006, China.

² Key Laboratory of Photonic Technology for Integrated Sensing and Communication, Ministry of Education of China, Guangdong University of Technology, Guangzhou, 510006, China.

³ Guangdong Provincial Key Laboratory of Information Photonic Technology, Guangdong University of Technology, Guangzhou 510006, China.

⁴ School of Optics and Electronics Information, Huazhong University of Science and Technology, Wuhan, 430074, China.

*songnian@gdut.edu.cn

Abstract

The mode-division multiplexing technique combined with a few-mode erbium-doped fiber amplifier (FM-EDFA) demonstrates significant potential for solving the capacity limitation of standard single-mode fiber (SSMF) transmission systems. However, the differential mode gain (DMG) arising in the FM-EDFA fundamentally limits its transmission capacity and length. Herein, an innovative DMG equalization strategy using femtosecond laser micromachining to adjust the refractive index (RI) is presented. Variable mode-dependent attenuations can be achieved according to the DMG profile of the FM-EDFA, enabling DMG equalization. To validate the proposed strategy, DMG equalization of the commonly used FM-EDFA configuration was investigated. Simulation results revealed that by optimizing both the length and RI modulation depth of the femtosecond laser-tailoring area, the maximum DMG (DMG_{\max}) among the three linear-polarized (LP) mode-group was mitigated from 10 dB to 1.52 dB, whereas the average DMG (DMG_{ave}) over the C-band was reduced from 8.95 dB to 0.78 dB. Finally, a 2-LP mode-group DMG equalizer was experimentally demonstrated, resulting in a reduction of the DMG_{\max} from 2.09 dB to 0.46 dB, and a reduction of DMG_{ave} over the C band from 1.64 dB to 0.26 dB, with only a 1.8-dB insertion loss. Moreover, a maximum range of variable DMG equalization was achieved with 5.4 dB, satisfying the requirements of the most commonly used 2-LP mode-group amplification scenarios.

Keywords: Mode-division multiplexing, Few-mode Erbium-doped fiber amplifier, Differential mode gain, Femtosecond laser micromachining

Introduction

Recently, various network applications such as artificial intelligence, the Internet of Things, virtual reality, and cloud computing are expected to rapidly deplete the transmission capacity based on standard single-mode fibers (SSMF). By extending the operation wavelength to the S-band, the SSMF-based transmission system has reached a capacity record of 206.1 Tb/s.¹ However, owing to the limitations originating from the fiber nonlinearity, further extending the transmission band to increase the capacity is not sustainable.² The mode-division multiplexing (MDM) technique, either by utilizing linear-polarized (LP) or the orbital angular momentum (OAM) mode as an independent transmission channel, has been regarded as a promising solution to mitigate the capacity limitations of traditional SSMF-based transmission systems.^{3,4} To deploy a long-haul MDM transmission system, a few-mode Erbium-doped fiber amplifier (FM-EDFA) with the ability to simultaneously amplify the wavelength division multiplexing (WDM) signals within all the guided modes is indispensable because the transmission attenuation of the few-mode fiber (FMF) needs to be compensated. Nevertheless, the differential modal gain (DMG) arising in the FM-EDFA owing to the different overlapping integrals among the pump mode profile, erbium doping, and signal mode profile, limits both the capacity and reach of the MDM transmission.^{5,6} Numerical results indicate that to achieve a 2000-km long-haul MDM transmission, an FMF link with a power variation of less than 1 dB is preferred.⁷

Several strategies have been proposed to minimize DMG, which can be divided into two categories. First, manipulation of the pump mode profile was implemented to achieve mode-selective Erbium-doped fiber (EDF) pumping.^{8,9} Alternatively, a cladding pumping scheme was proposed to homogenize the pump intensity within the core region.^{10,11} Second, the doping profile of the EDF was tailored to approach the optimal erbium ion distribution.¹²⁻¹⁴ These methods offer a DMG of less than 2 dB, but either a complicated pump configuration or a precise refractive index (RI) design of the FM-EDF is compulsory, increasing the deployment cost and inconvenience.

Because the DMG indicates the gain difference among all the guided modes, cascading a DMG equalizer with a variable mode-dependent attenuation after the FM-EDFA can significantly simplify the implementation of FM-EDFA. These DMG equalizers can be categorized into the following two types of configurations: free-space and all-fiber. Free-space DMG equalizers include spatial light modulators (SLM) and silica-based planar light-wave circuits (PLC). By utilizing the spatial attenuation of the SLM, a range of variable DMG equalizations of 10 dB and an insertion loss (IL) of 5 dB can be achieved within the LP₀₁ and LP₁₁ mode groups.¹⁵ However, 68% of the pumped power is expected to be dissipated. Meanwhile, a DMG equalizer based on a silica-based PLC with a 1.5 dB equalization range and 4 dB IL was demonstrated.¹⁶ Again, only 40% of the pumped power was efficiently used for optical amplification. Therefore, both free-space DMG equalizers suffer from high manufacturing costs and severe ILs. The high IL of this type of DMG equalizer reduces the minimum gain of the FM-EDFA over the C-band. Alternatively, the all-fiber configuration offers the benefits of a low IL, easy maintenance, and excellent compatibility. By splicing a short-segment, small-core, single-mode fiber between two FMFs, a DMG equalizer with an 8-dB equalization range and 2-dB IL was reported.¹⁷ A simulation study recently demonstrated that an all-fiber DMG equalizer based on cascaded long-period fiber gratings (LPGs) can reduce the DMG to lower than 0.6 dB. However, this requires both, specially designed fibers and several LPGs.¹⁸ Given the persistent need for an efficient approach to provide concise and effective DMG equalization, it is imperative to explore viable methods to fulfill this objective.

Femtosecond laser micromachining has gained research interest worldwide owing to its ability to achieve both localized and permanent RI tailoring in various transparent media.¹⁹⁻²¹ By manipulating the fabrication parameters, such as the pulse energy, laser repetition rate, and fabrication velocity, several functional optical devices have been successfully demonstrated, including Fabry-Perot interferometers,^{22,23} fiber gratings,²⁴⁻²⁷ light manipulators,²⁸⁻³⁰ and mode converters.^{31,32} These devices have been widely applied to optical communication and

sensing technologies.

In this study, a novel DMG equalization strategy based on in-line femtosecond laser micromachining that tailors the RI was proposed and experimentally demonstrated. Variable mode-dependent attenuation can be applied to each guided mode group by introducing an RI tailoring area into the FMF core, leading to successful DMG equalization. To verify the flexibility of the proposed DMG equalization strategy, a commonly used FM-EDFA with uniform erbium doping and fundamental-mode core-pumping was examined. First, when we numerically investigated the DMG increasing in the 3-LP mode-group FM-EDFA under variable pumping powers and EDF lengths, a detrimental DMG was identified. Subsequently, by optimizing the parameters of the DMG equalizer, including the femtosecond laser scanning length and width, and RI modification depth (Δn) induced by varying the femtosecond laser scanning times, a 3-LP mode-group DMG equalizer with a variable range of DMG equalization was obtained, which can be used to mitigate the DMG by cascading the all-fiber DMG equalizer after the FM-EDFA. Finally, a 2-LP mode-group DMG equalizer was experimentally fabricated via femtosecond laser micromachining, which can significantly reduce the DMG with a minimal insertion loss, and efficiently utilize the pumping power. Moreover, by modifying the scanning times of the femtosecond laser, the equalization range of the DMG equalizer can be efficiently adjusted to satisfy the requirements of the commonly used 2-LP mode-group FM-EDFA pumping configuration.

Results

DMG equalization strategy

Figure 1 presents a schematic of the proposed DMG equalization scheme. Various guided modes with the same launch power were transmitted over the FMF, and all the guided modes experienced nearly the same attenuation. However, when the FM-EDFA was used to compensate for the transmission attenuation, a DMG occurred, which is defined as the maximum gain difference between the guided modes at a

specific wavelength, as shown in equation (1)

$$DMG(\lambda) = \max_{m \neq n} |G(m, \lambda) - G(n, \lambda)| \quad (1)$$

where G is the gain value at the specific guide mode, λ is the operational wavelength, and m and n are the indices of the guided mode. Two metrics were defined to evaluate the performance of the DMG equalizer: DMG_{\max} and DMG_{ave} .

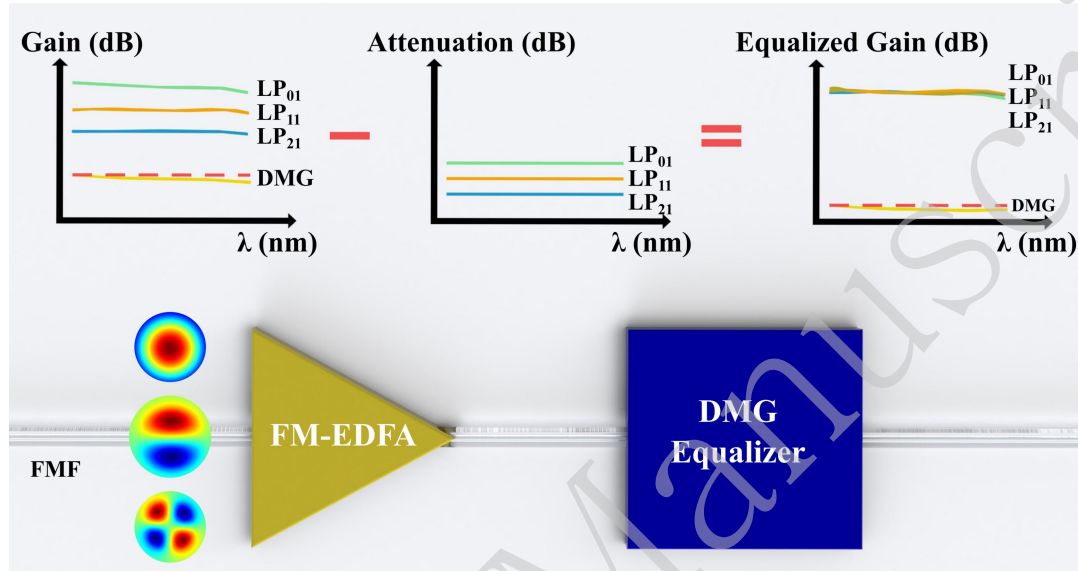


Figure 1. Schematic of the DMG-equalized FM-EDFA configuration.

The DMG_{\max} indicates the maximum DMG and DMG_{ave} is the average DMG in equation (1). Subsequently, to minimize the DMG, an in-line DMG equalizer with different mode attenuations (DMA) is cascaded after the FM-EDFA, and the DMA is defined as follows:

$$DMA(\lambda) = A_{LP_{01}}(\lambda) - A_{HOM}(\lambda) \quad (2)$$

where $A_{LP_{01}}$ is the attenuation of the LP_{01} mode and A_{HOM} is the attenuation of the high-order modes (HOMs). By modifying the RI of the FMF core via femtosecond laser micromachining, a higher attenuation is applied to the LP_{01} mode while minimizing its impact on the HOMs. Finally, the higher gain of the LP_{01} mode can be effectively reduced by cascading the fabricated DMG equalizer, consequently achieving the DMG equalization of the FM-EDFA.

Design of femtosecond laser micromachining-enabled DMG equalizer

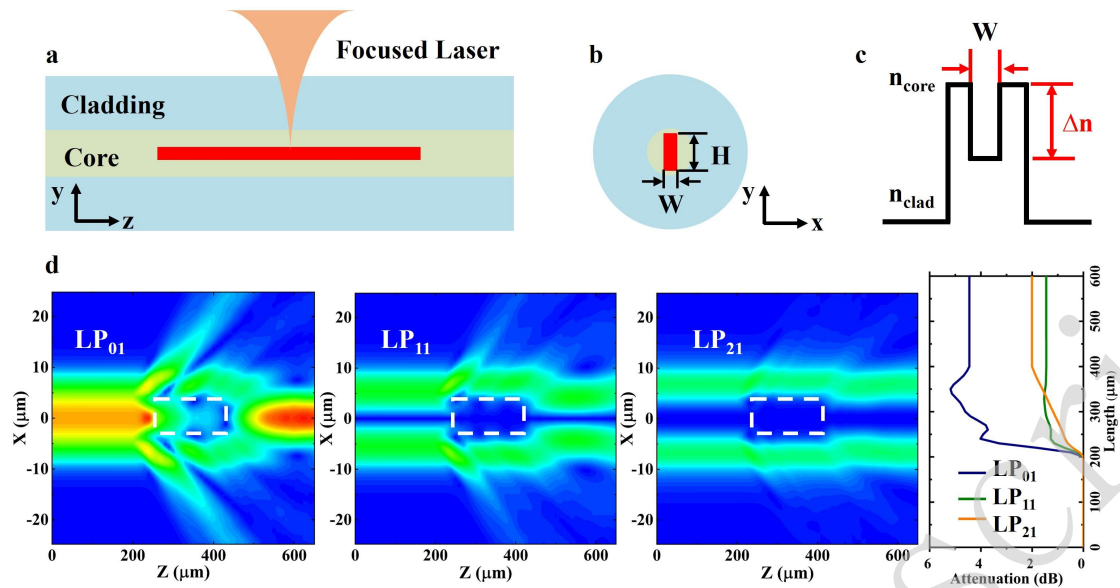


Figure 2. Schematic of the proposed DMG equalizer based on femtosecond laser micromachining. **a.** Schematic of the top-view of the modified RI region. **b.** Side view of the modified RI region. **c.** Modified RI profile following femtosecond laser micromachining. **d.** Simulation of the mode field and attenuation variations when different modes pass through the tailored RI region; the white dotted area indicates the modified RI region.

Figure 2(a) presents a schematic diagram of the proposed DMG equalizer. The femtosecond laser was focused on the core of the FMF to generate RI modulation. The modified RI region induced by the femtosecond laser was then modeled as a cuboid, whose width W , height H , length L , and RI modulation depth Δn can be flexibly manipulated by adjusting the femtosecond laser micromachining parameters, as shown in Fig. 2 (b) and (c). A simulation based on the beam propagation method was implemented to theoretically investigate the performance of the DMG, as shown in Fig. 2(d). Various guided modes are expected owing to leakage of the fiber cladding, consequently suffering different attenuations. The LP_{01} mode, whose profile is mainly concentrated at the center, experiences a larger attenuation than that of the HOMs. As shown in Fig. 2(d), different attenuations of the LP_{01} , LP_{11} , and LP_{21} modes were achieved by modeling a DMG equalizer in the FMF core. Because the degenerate modes are continuously and randomly coupled along the FMF, only the attenuation of the mode group is considered. Therefore, by optimizing the DMG equalizer parameters, the variable-mode-dependent attenuation among the various mode groups can be obtained. Finally, an all-fiber DMG equalizer with a variable range was anticipated.

Simulation results of 3-LP mode-group DMG equalizer

To verify the feasibility and advantages of the proposed DMG equalization strategy, a simple-structured and cost-effective 3-mode group EDFA with uniform Erbium doping and fundamental mode core-pumping was numerically investigated to introduce a larger DMG and identify the relationship between the DMG and pumping parameters, including the pumping power and EDF length, as shown in Fig. 3(a).

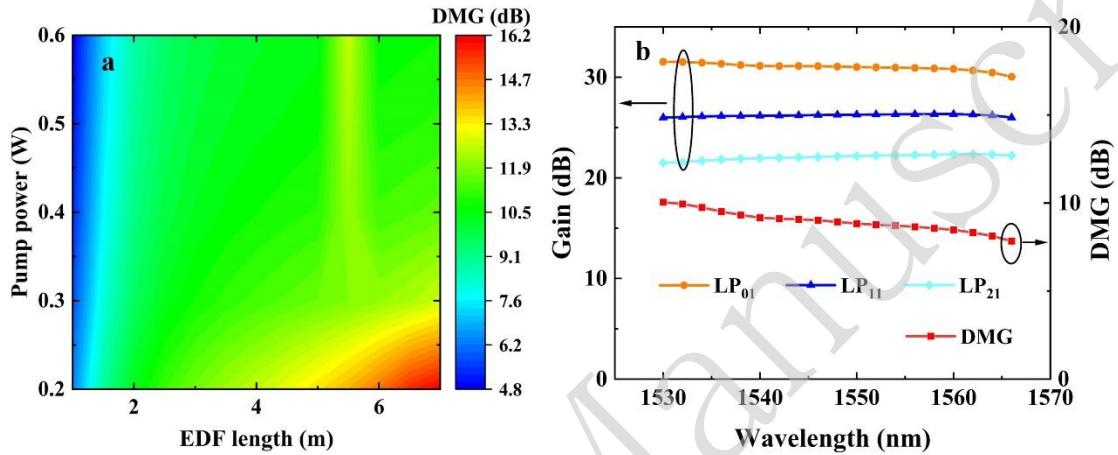


Figure 3. DMG arising in 3-LP mode group FM-EDFA. a. DMG under different pumping powers and lengths at 1550 nm. **b.** DMG over the C-band under the conditions of a 4.5-m EDF and 600 mW-fundamental mode pump.

As shown in Fig. 3(a), when the pumping power and EDF length were varied from 200 to 600 mW and 1 to 7 m, respectively, the DMG between the 3-mode groups fluctuated from 4.8 dB to 16.2 dB. Subsequently, an FM-EDFA configuration with a 4.5-m EDF and 600-mW fundamental mode pump power was selected to verify the DMG equalization process, where the DMG_{max} and DMG_{ave} over the C-band were 10 dB and 8.95 dB, respectively, as shown in Fig. 3(b).

The DMA of a 3-mode group DMG equalizer based on femtosecond laser micromachining to induce RI tailoring was numerically investigated. As shown in Fig. 4(a), when the L and Δn values vary from 0 to 400 μm and from 0 to -0.05, respectively, the DMA changes from 0 to 27.8 dB, which is sufficient to cover the entire DMG range of the 3-mode-group EDFA. Subsequently, the capability of the DMG equalization was numerically evaluated, as shown in Fig. 4(b).

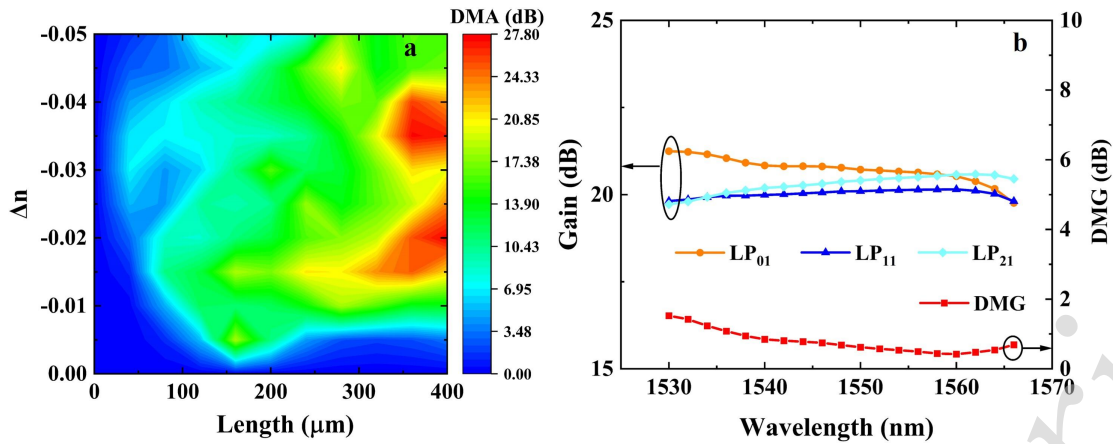


Figure 4. DMA introduced by the femtosecond laser micromachining-enabled RI tailoring. **a.** DMA of the 3-mode group DMG equalizer under different lengths and Δn values at 1550 nm. **b.** Gain profile when a DMG equalizer with a length of 120 μm and Δn of -0.02 was cascaded after the FM-EDFA.

Before DMG equalization, a 4.5 m EDF was core-pumped with a 600-mW, 980-nm laser in the fundamental mode, and the DMG_{max} and DMG_{ave} over the C-band were 10 dB and 8.95 dB, respectively. When a DMG equalizer with a length of 120 μm and Δn of -0.02 was cascaded after the designated FM-EDFA, the DMG_{max} decreased from 10 dB to 1.52 dB, and the average DMG_{ave} over the C-band decreased from 8.95 dB to 0.78 dB.

Discussion

As shown in Figure 5(a), the mode-dependent gain and DMG over the C-band of the 2-mode group before the DMG equalization was initially characterized owing to the lack of the 3-mode-group EDF. The maximum gains of the LP₀₁ and LP₁₁ mode groups were greater than 21 dB and 20 dB, whereas the DMG_{max} and DMG_{ave} values over the C-band were 2.09 dB and 1.68 dB, respectively. The variations in the DMG with the scanning length L were investigated, as shown in Figure 5(b). When the length L of the DMG equalizer gradually increased with an interval of 20 μm , the corresponding DMG_{max} and DMG_{ave} values after equalization were recorded under the different device lengths. When L increased from 0 to 300 μm , DMG_{max} gradually decreased from 2.09 dB to 0.46 dB, and DMG_{ave} decreased from 1.68 dB to 0.26 dB. Thus, the optimal length L was fixed at 300 μm . Subsequently, the scanning time N

was optimized, as

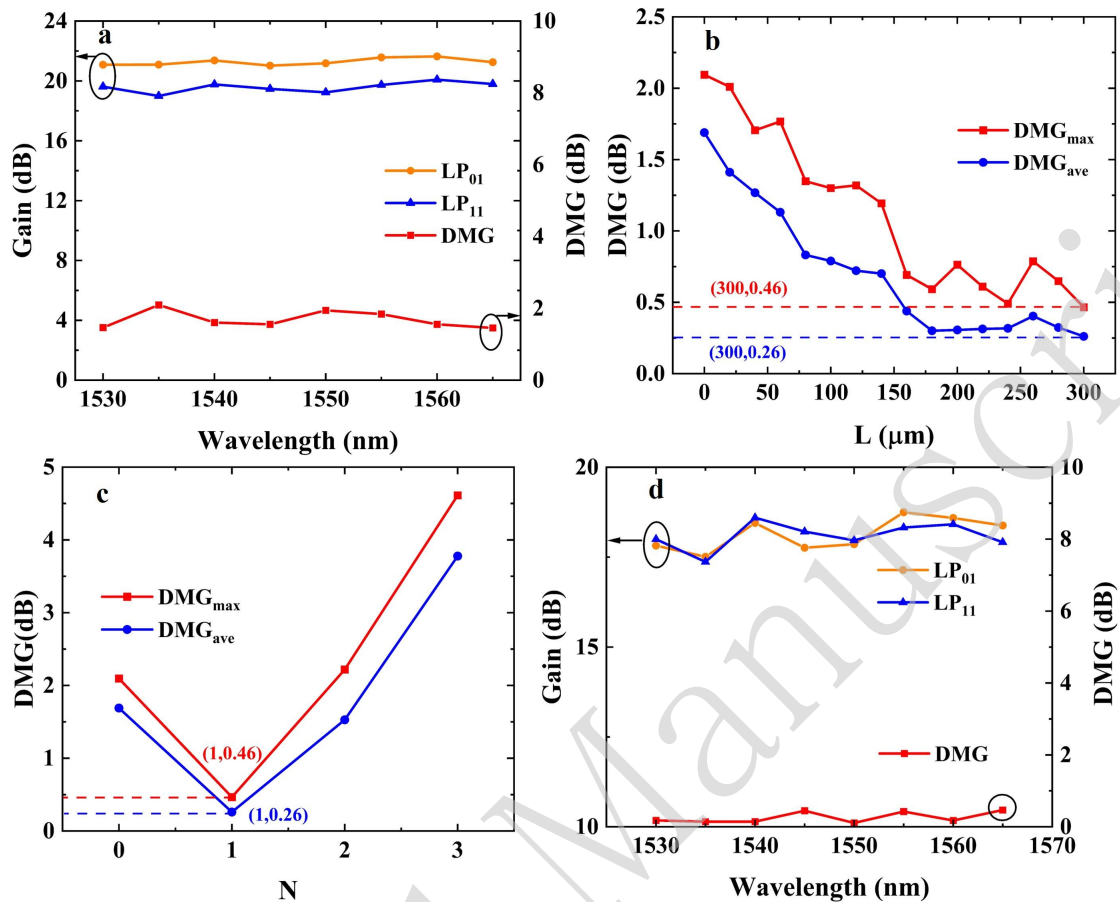


Figure 5. Characterization of the DMG equalization process. a. Modal gain and DMG over the C-band before DMG-equalization obtained from the experimental measurements. Variations in the measured DMG_{max} and DMG_{ave} with respect to: b. L, and c. the scanning times N. d. Experimentally measured modal gain and DMG over the C-band after DMG equalization.

shown in Figure 5(c). By increasing the femtosecond laser scanning time N, both DMG_{max} and DMG_{ave} increased, as a larger DMA occurred within the LP₀₁ and LP₁₁ mode groups. Therefore, the optimal value of both the length L and scanning times N were set to 300 μm and 1, respectively. Figure 5(d) presents the gain profile and DMG after equalization of the DMG with the optimal fabrication parameters. The values of DMG_{max} and DMG_{ave} decreased from 2.09 dB to 0.46 dB and from 1.64 dB to 0.26 dB, respectively. The maximum IL of the LP₁₁ mode group after using the DMG equalizer was less than 1.9 dB over the C-band, ensuring 64% utilization of the pump power.

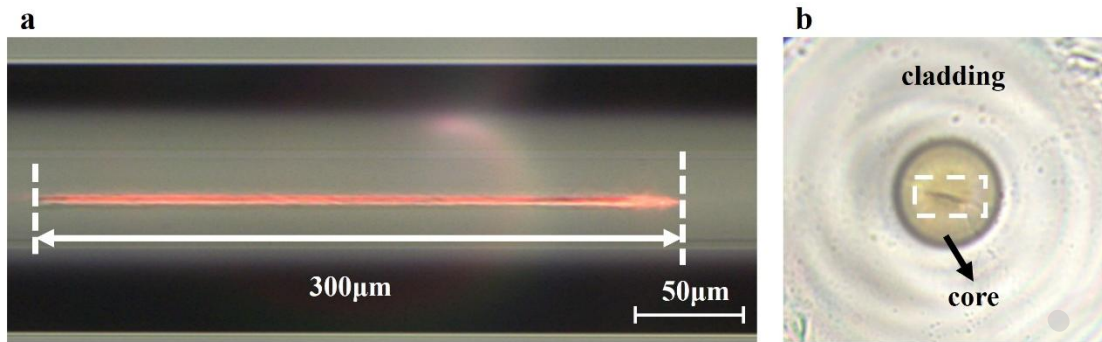


Figure 6. Microscopic image of the femtosecond laser micromachining-fabricated DMG equalizer. a. Top view; b. cross-sectional view.

A supercontinuum source (YSL Photonics) with an operational wavelength ranging from 450 to 2400 nm was launched into the FMF to obtain an intuitive vision of the inline DMG equalizer. Fig. 6(a) presents the top view of the DMG equalizer with a length of 300 μm after a single femtosecond laser scan captured by a camera. The fabricated DMG equalizer was then cleaved to obtain a cross-sectional view of the DMG equalizer, as shown in Fig. 6(b).

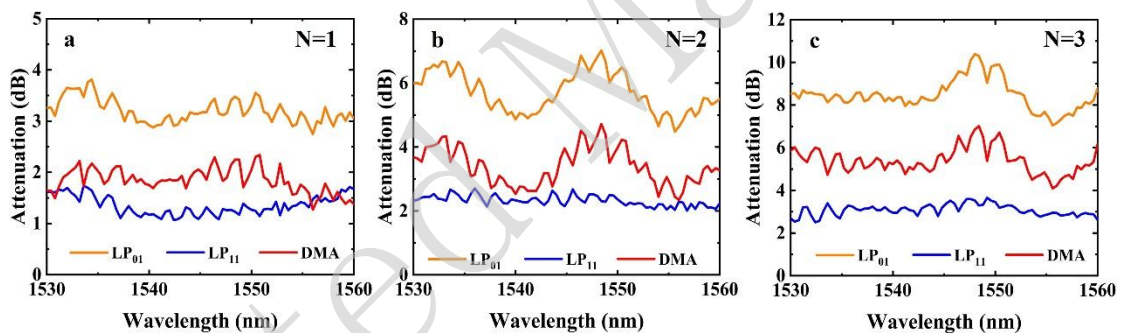


Figure 7. Relationship between the different attenuation modes with varied laser scanning times N . a. $N=1$. b. $N=2$. c. $N=3$.

Because the theoretical DMG of the 2-LP mode-group reached up to 6 dB, the range of the in-line DMG equalizer was investigated by changing the scanning times N , as shown in Fig 7. When $N=1$, the average attenuation of the DMG equalizer applied to the LP_{01} mode was approximately 3.14 dB, whereas the LP_{11} mode underwent an attenuation of 1.45 dB attenuation, leading to a 1.69-dB DMG equalization range. When $N=2$, the average attenuation values of the LP_{01} and LP_{11} mode groups are approximately 5.61 dB and 2.32 dB, respectively, resulting in a 3.29 dB range of DMG equalization. When $N=3$, the average attenuation value applied to

the LP₀₁ mode can reach 8.44 dB, introducing an additional attenuation of 3.05 dB to the LP₁₁ mode. Therefore, the maximum range of DMG equalization was obtained at 5.39 dB. By introducing the geometric parameters of the DMG equalizer into the simulation, the variation of Δn induced by a single scan was approximately -0.01. Further increasing the scanning time can extend the range of DMG equalization, but it also presents a severe IL to the LP₁₁ mode-group. In addition, the DMG equalizer introduced mode-crosstalk within the LP₁₁ mode-group, resulting in power oscillations. Both the IL and mode crosstalk of the LP₁₁ mode can be reduced with a more precise physical size control of the femtosecond laser-induced RI tailoring area.

In summary, we demonstrated an inline DMG equalizer based on femtosecond laser micromachining-induced RI tailoring. The Simulation results revealed that the optimizing parameters of the femtosecond laser micromachining, including both the length L and RI modulation depth Δn , can change the range of DMG equalization. To verify the correct function of our proposed equalization strategy, a commonly used FM-EDFA with both a uniform doping FM-EDF and fundamental-mode core pumping was used in both the simulation and experiment. The simulation results demonstrate that when the pump power and EDF length varied from 200 to 600 mW and from 1 to 7 m, the DMG within the LP₀₁, LP₁₁, and LP₂₁ mode groups varied from 4.8 dB to 16.2 dB. By cascading the DMG equalizer with optimal values of the length L and Δn , the values of DMG_{max} and DMG_{ave} over the C-band decreased from 10 dB to 1.52 dB and from 8.95 dB to 0.78 dB, respectively. Finally, a proof-of-concept experiment demonstrated that the DMG_{max} decreased from 2.09 dB to 0.46 dB, and the DMG_{ave} values over the C-band decreased from 1.64 dB to 0.26 dB. More importantly, the IL induced by the DMG equalization was less than 1.9 dB, indicating that 64% of the pumping power was efficiently utilized. The proposed DMG has a maximum equalization range of 5.4 dB, which satisfies the flexible application of the current FM-EDFA. A higher-order mode-group DMG equalization can be achieved with a more complicated RI modification pattern and higher-resolution femtosecond laser micromachining technology, which is ideally desirable for future long-haul MDM transmissions.

Materials and Methods

Experimental setup

The proposed DMG equalizer was fabricated using an ytterbium-doped femtosecond laser (Satsuma, Amplitude), which operated at a wavelength of 1030 nm, pulse width of 270 fs, and variable repetition frequency of 0-250 KHz. The laser was attenuated using a half-wave plate and a Glan prism before being focused onto the core of the FMF by a 20X objective (numerical aperture = 0.5). The FMF was positioned on a 3D motion stage (XMS-50, Newport) with a motion resolution of 50 nm. Real-time monitoring of the fabrication process and position reference of the laser focus plane were achieved when two CCDs were provided for the top and side views, respectively.

In addition, a real-time FM-EDFA mode-gain profile monitoring system was developed. The signal light from a multichannel tunable laser (TSP-1000, OVLINK) was fixed to -10 dBm for each mode group and co-propagated with a 980-nm pump light at a fundamental mode via a few-mode wavelength division multiplexer (FMSIWDM-15-900-1-FA, YX). Subsequently, the signal and pump light were introduced into a 5-m uniformly-doped FM-EDF with a doping concentration of 10^{25} m^{-3} . Two self-fabricated two-mode-group (LP_{01} and LP_{11}) photonic lanterns (PL) were used for mode-division multiplexing and demultiplexing. The state of polarization (SOP) of the light at the input port of PL_1 was carefully adjusted using a polarization controller (PC) to achieve the maximum output power at the same output port of PL_2 , and then fixed during fabrication and characterization. By conducting a measurement of the power transmission matrix of a pair of PLs, the mode crosstalk between the LP_{01} and LP_{11} mode groups was determined to be less than -13 dB. Finally, the spectra of the amplified signals were measured using an optical spectrum analyzer (OSA, AQ6370D, Yokogawa). Because the PL is mode-group-selective, the powers of the two LP_{11} output ports were summed as the power of the LP_{11} mode group. This real-time DMG monitoring ensures that the fabrication process achieves optimal DMG equalization.

Numerical simulation

Numerical computations of the DMG equalizer were performed using the beam-propagation method (BPM). The relationship between the parameters of the DMG equalizer and DMA was investigated. As shown in Fig. 2(d), the FMF used in the simulation had a step RI index with the same core/cladding diameter; the core RI was 1.4498 at 1550 nm. The white dotted area in Fig. 2(d) represents the DMG equalizer with a width of 4 μm , height of 13 μm , length of 120 μm , and Δn of -0.02. A cylinder with a bottom circular radius of 30 μm and height of 600 μm was set as the simulation region, which includes the DMG equalizer and corresponding input and output. The injection mode was the fiber mode of LP_{01} , LP_{11} , and LP_{21} respectively. Two degenerate modes (LP_{11a} and LP_{11b}) were individually injected into the simulation region and summed at the simulation output as one mode group.

The DMG of the 3-LP mode-group FM-EDFA was simulated based on the two energy levels of the EDFA model.³³ The influence of the pump power and FM-EDF length on the DMG was investigated, as shown in Fig. 3(a). The most commonly used pumping configurations of the fundamental-mode core pumping and FM-EDF with a step-index profile were used for the simulation. The FM-EDF used in the simulation had a step-index profile with a core/cladding diameter of 19/125 μm . The RI of the FMF core was 1.4507 at 1550 nm, and the erbium ions were uniformly doped at a concentration of 10^{25} m^{-3} . The passive FMF used in the simulation had a step RI index with the same core/cladding diameter; the core RI was 1.4498 at 1550 nm. To obtain the gain profile and DMG between the LP_{01} , LP_{11} , and LP_{21} mode groups under variable pumping powers and EDF lengths, the input signal power was fixed to -10 dBm for each mode group.

As shown in Fig. 4(a), the DMG equalizer used in the simulation had a width D and height H of 9 μm and 10 μm , respectively. The influence of the RI modulation depth Δn and length L on the DMA of DMG equalizer were investigated. To select the device parameters, the individual mode-group spectrum and DMG_{ave} over the C-band were first obtained. Subsequently, an equalizer with different parameters would introduce various mode-group attenuations. By subtracting the DMA spectrum from the un-equalized mode gain spectrum, the DMG over the C-band and

corresponding device parameters can be obtained, as shown in Fig. 4(b).

Device fabrication

The DMG was fabricated using femtosecond laser micromachining. The pulse energy and repetition frequency of the femtosecond laser were set to 1.8 μJ and 30 KHz, respectively. The 3D motion stage was programmed to scan along the FMF core axis with a speed of 10 $\mu\text{m/s}$ to fabricate the DMG equalizer.

Acknowledgements

This research was supported by the National Natural Science Foundation of China (62305071), China Postdoctoral Science Foundation (2023M740747), and Guangdong Introducing Innovative and Entrepreneurial Teams of “The Pearl River Talent Recruitment Program” (2021ZT09X044).

Author Contributions

C. Zhang conceived the idea and prepared the manuscript. S. Y. Zhang conducted the femtosecond laser micromachining process. Y. Zen prepared the FM-EDFA simulation results. Y. Wang conceived the schematic image. M. Xiang and Di Lin participated in the manuscript discussion. S. N. Fu and Y. W. Qin supervised and managed the entire project. All authors participated in the data analysis and contributed to writing the manuscript.

Conflict of interest

The authors declare no competing interests.

Supplementary information

Supplementary materials are available at the online version.

References

1. Puttnam, B. J. et al. S, C and extended L-band transmission with doped fiber and distributed Raman amplification. 2021 Optical Fiber

- Communications Conference and Exhibition (OFC). San Francisco: IEEE, 2021, 1-3.
2. Winzer, P. J., Neilson, D. T. & Chraplyvy, A. R. Fiber-optic transmission and networking: the previous 20 and the next 20 years [Invited]. *Optics Express* **26**, 24190-24239 (2018).
 3. Richardson, D. J., Fini, J. M. & Nelson, L. E. Space-division multiplexing in optical fibres. *Nature Photonics* **7**, 354-362 (2013).
 4. Bozinovic, N. et al. Terabit-scale orbital angular momentum mode division multiplexing in fibers. *Science* **340**, 1545-1548 (2013).
 5. Mello, D. A. A. et al. Impact of Polarization- and mode-dependent gain on the capacity of ultra-long-haul systems. *Journal of Lightwave Technology* **38**, 303-318 (2020).
 6. Sillard, P. et al. Few-mode fiber technology, deployments, and systems. *Proceedings of the IEEE* **110**, 1804-1820 (2022).
 7. Ip, E. et al. Impact of mode-dependent loss on long-haul transmission systems using few-mode fibers. 2016 Optical Fiber Communications Conference and Exhibition (OFC). Anaheim: IEEE, 2016, 1-3.
 8. Bai, N. et al. Multimode fiber amplifier with tunable modal gain using a reconfigurable multimode pump. *Optics Express* **19**, 16601-16611 (2011).
 9. Lopez-Galmiche, G. et al. Few-mode erbium-doped fiber amplifier with photonic lantern for pump spatial mode control. *Optics Letters* **41**, 2588-2591 (2016).
 10. Jung, Y. et al. Cladding pumped few-mode EDFA for mode division multiplexed transmission. *Optics Express* **22**, 29008-29013 (2014).
 11. Chen, H. et al. Integrated cladding-pumped multicore few-mode erbium-doped fibre amplifier for space-division-multiplexed communications. *Nature Photonics* **10**, 529-533 (2016).
 12. Kang, Q. Y. et al. Accurate modal gain control in a multimode erbium doped fiber amplifier incorporating ring doping and a simple LP₀₁ pump configuration. *Optics Express* **20**, 20835-20843 (2012).
 13. Genevaux, P. et al. A five-mode erbium-doped fiber amplifier for mode-division multiplexing transmission. *Journal of Lightwave Technology* **34**, 456-462 (2016).

14. Li, Z. Q. et al. Amplification and transmission system with matching multi-layer ion-doped FM-EDFA. *Journal of Lightwave Technology* **41**, 695-701 (2023).
15. Blau, M. et al. Variable optical attenuator and dynamic mode group equalizer for few mode fibers. *Optics Express* **22**, 30520-30527 (2014).
16. Fujisawa, T. et al. Silica-PLC based mode-dependent-loss equalizer for two LP mode transmission. 2022 Optical Fiber Communications Conference and Exhibition (OFC). San Diego: IEEE, 2022, 1-3.
17. Jung, Y., Alam, S. U. & Richardson, D J. All-fiber spatial mode selective filter for compensating mode dependent loss in MDM transmission systems. 2015 Optical Fiber Communications Conference and Exhibition (OFC). Los Angeles: IEEE, 2015, 1-3.
18. Zhu, J. L. et al. Few-mode gain-flattening filter using LPFG in weakly-coupled double-cladding FMF. *Journal of Lightwave Technology* **39**, 4439-4446 (2021).
19. Beresna, M., Gecevičius, M. & Kazansky, P. G. Ultrafast laser direct writing and nanostructuring in transparent materials. *Advances in Optics and Photonics* **6**, 293-339 (2014).
20. Jia, Y. C., Wang, S. X. & Chen, F. Femtosecond laser direct writing of flexibly configured waveguide geometries in optical crystals: fabrication and application. *Opto-Electronic Advances* **3**, 190042 (2020).
21. Tan, D. Z. et al. Photonic circuits written by femtosecond laser in glass: improved fabrication and recent progress in photonic devices. *Advanced Photonics* **3**, 024002 (2021).
22. Li, C. X. et al. Femtosecond laser direct writing of a 3D microcantilever on the tip of an optical fiber sensor for on-chip optofluidic sensing. *Lab on a Chip* **22**, 3734-3743 (2022).
23. Zhao, Y. et al. Femtosecond laser-inscribed fiber-optic sensor for seawater salinity and temperature measurements. *Sensors and Actuators B: Chemical* **353**, 131134 (2022).
24. Dash, J. N. et al. Rectangular single-mode polymer optical fiber for femtosecond laser inscription of FBGs. *Photonics Research* **9**, 1931-1938 (2021).

25. Wolf, A. et al. Advances in femtosecond laser direct writing of fiber Bragg gratings in multicore fibers: technology, sensor and laser applications. *Opto-Electronic Advances* **5**, 210055 (2022).
26. Yang, C. L. et al. Mode converter with C+L band coverage based on the femtosecond laser inscribed long period fiber grating. *Optics Letters* **46**, 3340-3343 (2021).
27. Jiang, C. et al. Femtosecond laser inscribed parallel long-period fiber gratings for multi-channel core mode conversion. *Optics Letters* **47**, 3207-3210 (2022).
28. Sakakura, M. et al. Ultralow-loss geometric phase and polarization shaping by ultrafast laser writing in silica glass. *Light: Science & Applications* **9**, 15 (2020).
29. Reupert, A. et al. Angular scattering pattern of femtosecond laser-induced refractive index modifications in optical fibers. *Advanced Optical Materials* **8**, 2000633 (2020).
30. Lu, J. F. et al. Tailoring chiral optical properties by femtosecond laser direct writing in silica. *Light: Science & Applications* **12**, 46 (2023).
31. Zhang, C. et al. Femtosecond laser micro-machining enabled all-fiber mode selective converter. *Optics Letters* **44**, 5941-5944 (2019).
32. Li, Y. L. et al. High purity optical vortex generation in a fiber Bragg grating inscribed by a femtosecond laser. *Optics Letters* **45**, 6679-6682 (2020).
33. Giles, C. R. & Desurvire, E. Modeling Erbium-doped fiber amplifiers. *Journal of Lightwave Technology* **9**, 271-283 (1991).